Future Resource Studies in the MISO System

By Lei Wu, Yikui Liu, Yafei Yang and Yonghong Chen
ECE Department, Stevens Institute of Technology and MISO R&D

September 6, 2020

MISO

Table of Contents

Table of Figures

Table of Tables

Executive Summary

From October 2019 to August 2020, MISO Research and Development (R&D) partnered with the Stevens Institute of Technology (SIT) to study what would be needed to effectively integrate distributed energy resources (DERs) into MISO power system operations and market clearing, and to explore options to address potential issues. This report highlights findings and relevant test results and suggests potential directions that might be worth further exploration in future work.

The research focused on the following three areas:

A1. If and how limited coordination between generation and load-responsive DERs and wholesale markets might induce oscillation in locational marginal price (LMP) and/or transmission flow

A2. Whether novel algorithmic approaches of grouping elemental pricing nodes (Epnodes) with similar impacts on network security constraints might improve unit commitment (UC) computational performance

A3. What transmission and distribution coordination approaches might be effective in mitigating any risks

This study arrived at three preliminary observations:

O1. **Locational Marginal Price (LMP) and/or transmission flow oscillation may not be avoidable under current aggregation approaches across multiple Epnodes**. Oscillation in LMP and/or transmission flows can occur if the elasticity and locational response of DERs are not precisely known and modeled in grid operators' unit commitment (UC) and economic dispatch (ED) models. Scenarios that can lead to errors in elasticity include:

(i) DER offers may not reflect their true price elasticity
(ii) Distribution factors used by MISO in the UC and ED model to represent DER aggregations may not be consistent with aggregations' actual responses
(iii) Supply-side and demand-side DERs may deviate from market clearing instructions if distribution-level physical and operational constraints become binding

These unanticipated responses can trigger unexpected transmission constraints or change the shadow prices of transmission constraints, leading to LMP oscillation across pricing intervals. LMP oscillation is often associated with transmission flow oscillation that may cause flows to exceed limits and introduce reliability risk. Based on extensive preliminary testing of current aggregation approaches across EPnodes, the aggregate DER may perfectly follow the total MW dispatch instruction from the Regional Transmission Operator (RTO). However, if the offered aggregate price curves and distribution factors do not accurately reflect the elasticity of individual assets under the aggregation, the actual responses from individual Epnode locations may be inconsistent with the market clearing solution, driving LMP or flow oscillation and even unexpected violation of flow limits at times.

O2. **Integrating large numbers of DER into the market introduces computational challenges. However, a novel algorithmic approach of grouping like EPNodes could help improve computational performance**. Allowing aggregation across multiple Epnodes in the market rule may help reduce the total number of dispatchable resources in the security-constrained unit commitment (SCUC) optimization model. Limiting DER aggregation on single Epnode in the market rule may result in larger number of variables and associated non-zero coefficients in network security constraints of SCUC. Indeed, more variables and a denser coefficient matrix of network security constraints will result in a longer time to solve linear programming (LP) sub-problems within the mixed-integer linear programming (MILP)-based SCUC computation. To address

these computing challenges, the team developed novel approaches to potentially group pnodes with similar impacts within the optimization to reduce the number of variables and non-zero coefficients in the network security constraints. These approaches could improve the performance of SCUC with DER participating at the Epnode level and derive high-quality UC solutions within the solution time limit.

O3. **Novel coordination approaches for Epnode-level aggregation appear to guarantee the operational feasibility of distribution systems, achieve sufficiently good dispatch solutions that are close to the ideal transmission-distribution co-optimization solution, and avoid LMP oscillation**. The team explored two transmission and distribution coordination approaches for integrating DERs at the Epnode level that could improve coordination by reflecting the operational and physical characteristics of DERs and the distribution systems. Both require projection but have different data requirements. However, the potential coordination approaches examined require more information and extra data exchange and model changes for transmission and distribution grid operators. MISO will continue to research efficient ways to integrate DER.

These research findings indicate that accurate locational information about DER aggregations' responses to dispatch is necessary for the efficient and reliable operations of the Bulk Electric System. Aggregation at the Epnode is the preferred method to limit oscillation concerns, while MISO conducts additional research on other potential methods. In addition, because the potential coordination approaches examined require more information and extra data exchange and model changes for grid operators, the team is further investigating whether alternate control strategies could avoid or mitigate oscillation while also deriving sufficiently good dispatch solutions. The team continues to investigate alternative ways to improve computational performance through grouping and other techniques within the solution process.

Additional technical detail about the research is available through a series of publications found in Section 5: References.

1. LMP Oscillation Studies Induced by DERs

To assess the potential for LMP oscillation due to limited DER coordination, the team analyzed two scenarios:

(i) Price responsive demands (PRD) treated as "fixed" loads in the market clearing model, which iteratively adjust to LMPs from the market clearing results
(ii) DERs aggregated at the commercial pricing node (Cpnode) level using approximated distribution factors

Under both of these scenarios, simulation indicates that LMP oscillation can present in the real-time market clearing process when the actual DER response quantity or locations do not match what is represented in the market clearing solution. This could occur where:

(i) DER offers may not reflect their true price elasticity
(ii) Distribution factors used by MISO in the UC and ED model to represent DER aggregations may not be consistent with aggregations' actual responses
(iii) Supply-side and demand-side DERs may deviate from market clearing instructions if distribution-level physical and operational constraints become binding

Aggregation a the EPnode would limit this oscillation as compared to aggregation at the commercial pricing node level. As such, while MISO researches alternative approaches, MISO recommends aggregating DERs at the Epnode level.

1.1. PRDs Treated as "Fixed" Loads

Figure 1 shows the iterative simulation procedure when PRDs are modelled as "fixed" loads in the wholesale real time market clearing process similar to current practice. Specifically, PRDs are considered as fixed loads in the UC and ED model for market clearing; then PRDs adjust their load levels according to LMPs and their individual load elasticity curves. The adjusted PRD quantity is reflected in state estimation and the state estimation snapshot is used for the next iteration. The iterative procedure exhibits the dynamic interactions between the market and PRDs. The team considered two strategies for the UC and ED market clearing model: (i) UC results are re-optimized with respect to new load levels; and (ii) UC results are fixed and only ED is re-optimized. Five typical load elasticity curves are considered (Figure 1).

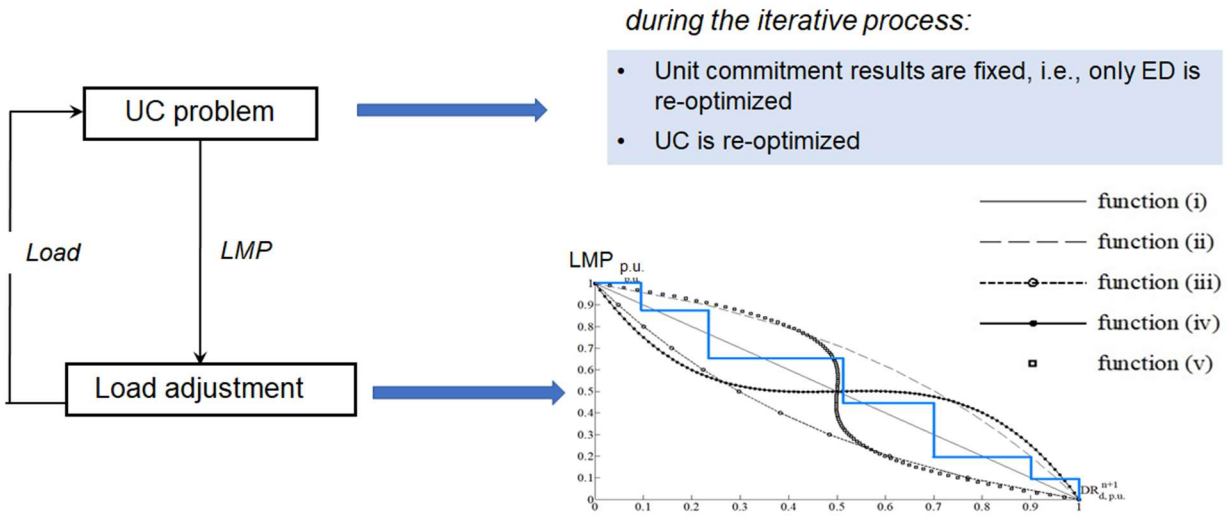

Figure 1: The iterative simulation procedure when PRDs are considered as "fixed" loads.

Figure 2 illustrates the test results on a day-ahead MISO case modified from with different PRD penetration levels. It shows that LMP oscillation are more severe with a higher PRD penetration level (i.e., 10% versus 5%) under the same elasticity assumption and no new coordination approaches. A higher PRD penetration level induces larger load deviations in two consecutive runs, leading to more significant LMP oscillation.

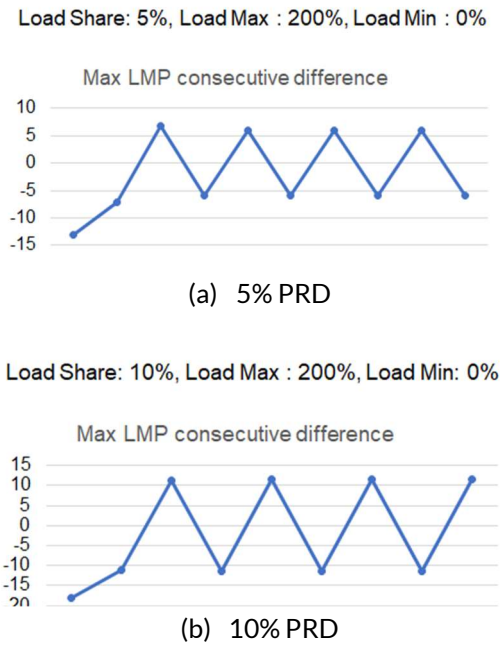

Figure 2: LMP oscillations against different PRD penetration levels.

Figure 3 shows the test results with different UC and ED execution strategies. When UC is re-optimized with respect to new load levels as a result of the response of PRDs, LMP oscillations become more severe. When UC is re-optimized with respect to new load levels, the new UC solution attempts to make the best utilization of available system resources, which could induce new binding transmission constraints. To this end, the new binding transmission constraints and their corresponding shadow prices could drive more significant oscillation in LMPs.

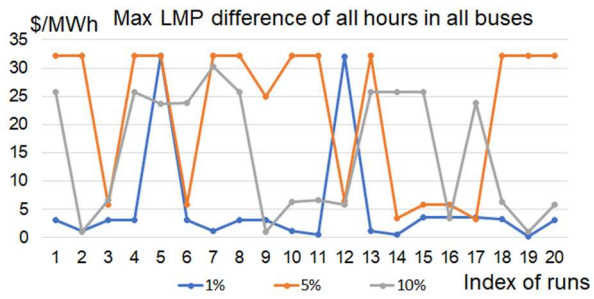

(a) Reoptimize UC

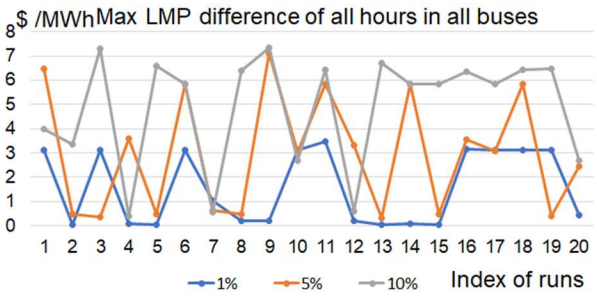

(b) Reoptimize ED with fixed UC solutions

Figure 3: LMP oscillations against different UC/ED execution strategies.

These studies clearly show that LMP oscillation is unavoidable if PRDs are treated as fixed loads in the UC and ED model. While treating PRDs as fixed loads is an extreme case, the analysis indicates the outcome of not representing true price elasticity in the market clearing model.

1.2. DERs are Aggregated at the Cpnode Level Using Approximated Distribution Factors

Figure 4 shows the iterative processes used to simulate DER aggregation at CPnode with approximated distribution factors. The study considered three strategies for updating distribution factors:

- **Case 1.** The distribution factor is updated in each real-time economic dispatch (RTED) iteration based on the most recent state estimation (SE) results
- **Case 2**. The distribution factor update is delayed by certain intervals to help mitigate oscillation
- **Case 3.** The distribution factor is fixed (i.e., never updated)

This analysis assumes that DERs respond to the RTED dispatch target MW perfectly. The allocation of the dispatch target MW to Epnodes is economically determined by the aggregators and does not necessarily align with the distribution factors used in RTED. Also, the distribution factor is the single difference among individual RTED runs, while all other parameters remain the same.

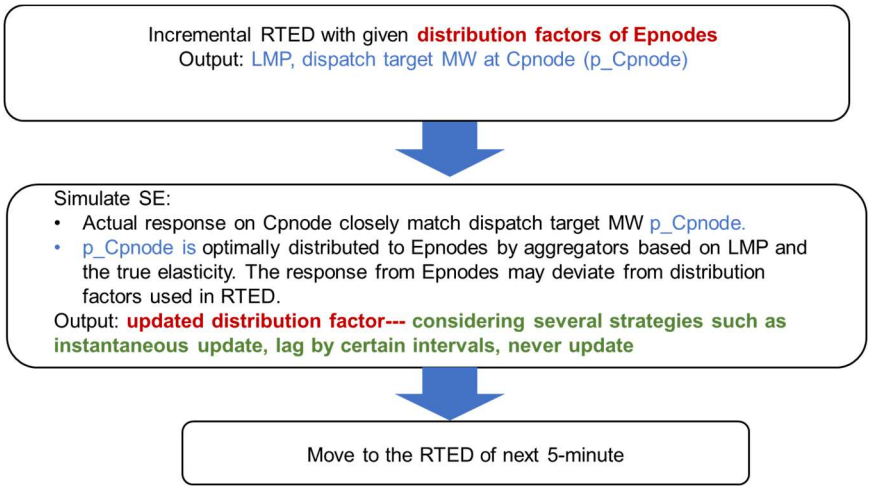

Figure 4: Iterative simulation procedure when DERs are simulated via distribution factors.

A small system illustrates the LMP oscillation phenomena (Figure 5) under these scenarios. The transmission network (blue) has generators, P_1 and P_2, and one fixed load, L. The connected distribution networks (red) have two DERs (i.e., generation resources with real power injections DER_1 and DER_2) and participate in the wholesale market via a Cpnode using approximated distribution factors.

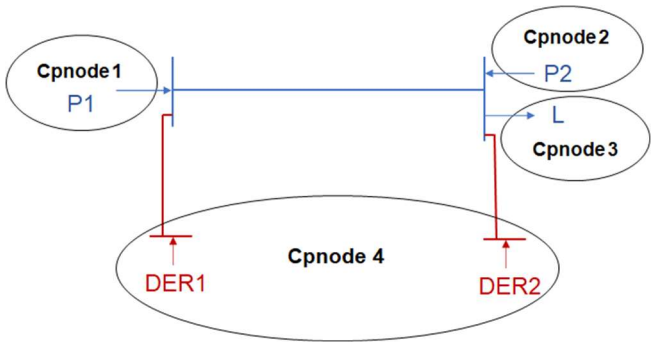

Figure 5: A small system for LMP oscillation illustration.

The results show that *LMP oscillation occurs* in all cases (Tables 1, 2 and 3). In Case 1, LMP oscillation is mainly caused by oscillating distribution factors of the two DERs, which switches the binding status of the transmission line to be active and inactive in a cyclic manner.

Case 2 shows that when distribution factor update is delayed by one interval, the *oscillation cycle is enlarged*. In addition, as the other parameters for the incremental RTED (i.e., the remaining available transmission capacity obtained by last SE) and distribution factors are not synchronized, scheduled transmission line flows in certain RTED intervals (e.g., interval 6) could *be higher than the limit* (which is 100.75MW in our study).

Case 3 is considered as an extreme situation of Case 2, in which the distribution factor update cycle is infinite (i.e., never updated). LMP oscillation is still observed, and transmission line flow violations (i.e., higher than the limit) are observed more frequently.

This study also explored other distribution factor update strategies, such as the weighted sum of the most recent several distribution factors. However, these approaches could be considered as combinations or extensions of the strategies adopted in Cases 1 and 2. There is always a case that presents LMP oscillation as long as the actual response does not match the distribution factors used to generate the RTED target dispatch solution.

	Time	1	2	3	4	5	6	7	8
Real Time Economic Dispatch	Generator P_1 (MW)	100	100	100	98.5	100	98.5	100	98.5
	Generator P_2(MW)	5	2	5	3.5	5	3.5	5	3.5
	DER 1 (MW)	0	3	0	3	0	3	0	3
	DER 2 (MW)	1	1	1	1	1	1	1	1
	Transmission line flow (MW)	100.75	100	100.75	98.5	100.75	98.5	100.75	98.5
	Distribution factor	0.75	0	0.75	0	0.75	0	0.75	0
	LMP of CPnode 4 ($/MWh)	8.5	16	8.5	16	8.5	16	8.5	16
State Estimation	Generator P_1 (MW)	100	97.75	100	97.75	100	97.75	100	97.75
	Generator P_2 (MW)	5	4.25	5	4.25	5	4.25	5	4.25
	DER 1 (MW)	0	3	0	3	0	3	0	3
	DER 2 (MW)	1	1	1	1	1	1	1	1
	Transmission line flow (MW)	100	100.75	100	100.75	100	100.75	100	100.75

Table 1: Results of Case 1

	Time	1	2	3	4	5	6	7	8
Real Time Economic Dispatch	Generator P_1 (MW)	100	100	100	100	100	100	100	100
	Generator P_2 (MW)	5	5	2	2	5	4	2	5
	DER 1 (MW)	0	0	3	3	0	1	3	0
	DER 2 (MW)	1	1	1	1	1	1	1	1
	Transmission line flow (MW)	100.75	100.75	100	100	100.75	101.5	100	100.75
	Distribution factor	0.75	0.75	0	0	0.75	0.75	0	0
	LMP of CPnode 4 ($/MWh)	8.5	8.5	16	16	8.5	12	16	12
State Estimation	Generator P_1 (MW)	100	100	100	97.75	97.75	100	99.75	97.75
	Generator P_2 (MW)	6	5	5	4.25	4.25	5	4.25	4.25
	DER 1 (MW)	0	0	0	3	3	0	1	3
	DER 2 (MW)	0	1	1	1	1	1	1	1
	Transmission line flow (MW)	100	100	100.75	100.75	100	100.75	100.75	100.5

Table 2: Results of Case 2

	Time	1	2	3	4	5	6	7	8
Real Time Economic Dispatch	Generator P_1 (MW)	100	100	100	100	100	100	100	100
	Generator P_2 (MW)	5	5	4	5	3.33	5	3.56	5
	$DER1$ (MW)	0	0	1	0	1.67	0	1.44	0
	$DER2$ (MW)	1	1	1	1	1	1	1	1
	Transmission line flow (MW)	100.75	100.75	101.5	100.75	102	100.75	101.83	100.75
	Distribution factor	0.75	0.75	0.75	0.75	0.75	0.75	0.75	0.75
	LMP of CPnode 4 ($/MWh)	8.5	8.5	12	8.5	12	8.5	12	8.5
State Estimation	Generator P_1 (MW)	100	100	100	99.75	100	99.08	100	99.31
	Generator P_2 (MW)	6	5	5	4.25	5	4.25	5	4.25
	DER 1 (MW)	0	0	0	1	0	1.67	0	1.44
	DER 2 (MW)	0	1	1	1	1	1	1	1
	Transmission line flow (MW)	100	100	100.75	100	100.75	100	100.75	100

Table 3: Results of Case 3

2. Approaches to Group Epnodes for Transmission Constraints

When the study simulated DERs participating at the Epnode level throughout the grid, the number of Epnodes with DERs and, consequently, the number of non-zero coefficients in the network security constraints of SCUC, increase significantly. The network security constraints in the day-ahead market model are currently formulated at the master pnode level, by aggregating Cpnodes with the same shift factor (SF) value. With this, if a large number of DERs participate in the Epnode level and result in a significant increase of the number of Cpnodes, the number of master pnodes can be too large for SCUC to solve within an acceptable time limit. Therefore, the team explored a grouping approach to further reduce the variables in network security constraints and improve the SCUC performance.

First, a clustering method is developed to group master pnodes with similar SFs. The grouped master pnodes are referred to as similar pnodes. Figure 6 shows the relationship between Epnodes, master pnodes, and similar pnodes. Next, the network security constraints are represented by similar pnodes grouped with reduced number of non-zeros. The SCUC with network security constraints represented by similar pnodes can be solved efficiently and derive sufficiently good UC solutions. Solution qualities are evaluated by recalculating SCED with respect to UC solutions and original network security constraints (i.e., without similar pnode grouping).

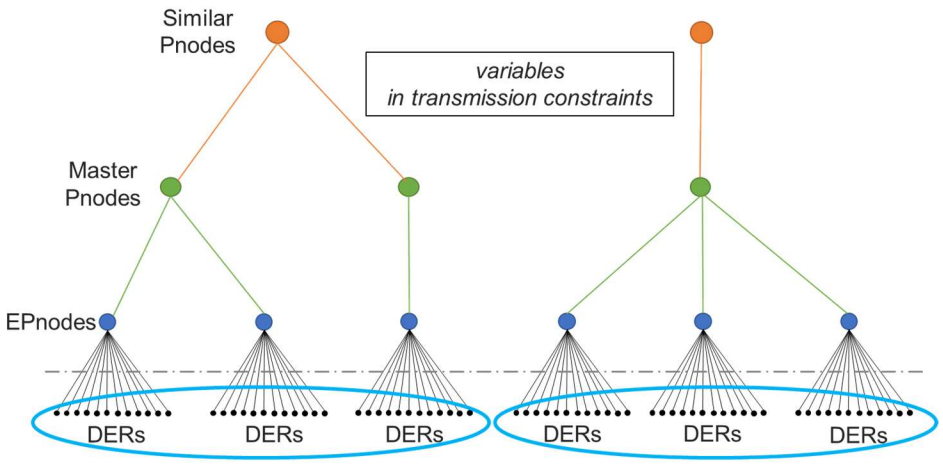

Figure 6: Relationship between Epnodes, Master Pnodes, and Similar Pnodes

2.1. Variable Grouping for Network Security Constraints

The key issues of variable grouping include: (i) defining a metric for similarity evaluation, and (ii) designing an efficient clustering procedure. The similarity index (SI) between two master pnodes is defined as the maximum absolute difference between the two SF vectors of master pnodes (Equation 1), where SF_{l,n_i} is the shift factor of the power flow on branch l to the power injection on node n_i.

$$SI_{n_i,n_j} = \max_l \left| SF_{l,n_i} - SF_{l,n_j} \right|, n_i \neq n_j$$

Equation 1

With a pre-defined similarity threshold ε_{SI}, the procedure to cluster variables in network security constraints is summarized as:

1. Calculate $SI_{n1,n2}$ for each pair of $n1, n2 \in \{1, \dots, N\}$ and $n1 \neq n2$
2. Form an undirected graph $(\mathbb{V}, \mathbb{E})$ with the vertex set $\mathbb{V} = \{1, \dots, N\}$ and edge set $\mathbb{E} = \{(n1, n2): SI_{n1,n2} \leq \varepsilon_{SI}\}$
3. Find all exclusive complete subgraphs in graph $(\mathbb{V}, \mathbb{E})$

The variable grouping with a smaller ε_{SI} will be more accurate, while a larger ε_{SI} results in fewer similar pnodes and consequently result in a higher computational efficiency. The grouping results with different similarity thresholds are presented in Table 4. With $\boldsymbol{\varepsilon_{SI}}$=0.02 or 0.03, the numbers of pnodes after grouping are similar and significantly less than the number of master pnodes in existing systems. The impact of different ε_{SI} values on SCUC performance and solution quality will be explored in Section 2.3: Case Studies.

Similarity threshold ε_{SI}	Number of nodes	
	Case A	Case B
$\varepsilon_{SI} = 0$ (Epnodes)	14,397	14,262
ε_{SI} =1e-6 (MasterPnodes)	7,114	7,069
$\varepsilon_{SI} = 0.01$ (Similar Pnodes)	2,587	2,880
$\varepsilon_{SI} = 0.02$ (Similar Pnodes)	1,554	1,781
$\varepsilon_{SI} = 0.03$ (Similar Pnodes)	1,130	1,316

Table 4:Results of grouping with different similarity thresholds

2.2. SCUC Solution Procedure

Figure 7 shows the proposed SCUC solution procedure. The first step clusters variables and constructs grouped network security constraints. Next, the grouped network security constraints are used to obtain the UC solution. Finally, with the given UC solution, economic dispatch and LMPs are solved by SCED with the original network security constraints. It is noteworthy that with the fixed UC solution obtained in Step 2, SCED in Step 3 will satisfy the original network security constraints through re-dispatch. Numerical tests show that, with a grouping of high accuracy, the objective value obtained from Step 3 would be reasonably close to that of the original SCUC (i.e., the SCUC model without similar pnode grouping).

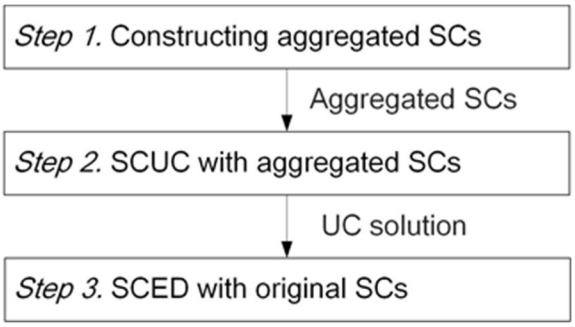

Figure 7: Flowchart of SCUC via grouped network security constraints (NSC)

The basic idea of constructing grouped network security constraints can be illustrated by a two-dimensional example (Figure 8). The original constraint is $l: P_1/a_1 + P_2/a_2 \leq 1, with\ a_1 \geq a_2$, which will be grouped and reformulated as $\tilde{l}: \tilde{a} \cdot \tilde{P} \leq \tilde{b}$ and $\tilde{P} = P_1 + P_2$. A proper $\tilde{a}$ shall be in $[1/a_1, 1/a_2]$, which can be used to obtain two grouped constraints $l_1: (P_1 + P_2)/a_1 \leq 1$ and $l_2: (P_1 + P_2)/a_2 \leq 1$.

If resource capacity limits $0 \leq P_1 \leq \bar{P}_1$ and $0 \leq P_2 \leq \bar{P}_2$ are further considered, two other grouped constraints $l_3: (P_1 + P_2)/a_1 \leq 1 - \Delta|_{\tilde{a}=a_1} = 1 - (a_1 - a_2)\bar{P}_2/a_1 a_2$ and $l_4: (P_1 + P_2)/a_2, \leq 1 + \Delta|_{\tilde{a}=a_2} = 1 + (a_1 - a_2)\bar{P}_1/a_1 a_2$ can be obtained, where Δ is the grouping error with respect to $\tilde{a}$.

Figure 8 shows that l_2 and l_4 reduce the feasible region of the original problem (i.e., a conservative grouping), while l_1 and l_3 enlarge the feasible region (i.e., a relaxed grouping). Suppose l is a binding constraint and the optimal solution of the original SCUC lies between points o_1 and o_2, both l_3 and l_4 have the same maximum possible distance (i.e., the distance between l_3 and l_4) to the original optimal solution. To this end, to obtain good near-optimal solutions to the original problem and to balance conservative and relaxed groupings, a proper grouped constraint $\tilde{l}$ could be at the middle position between l_3 and l_4.

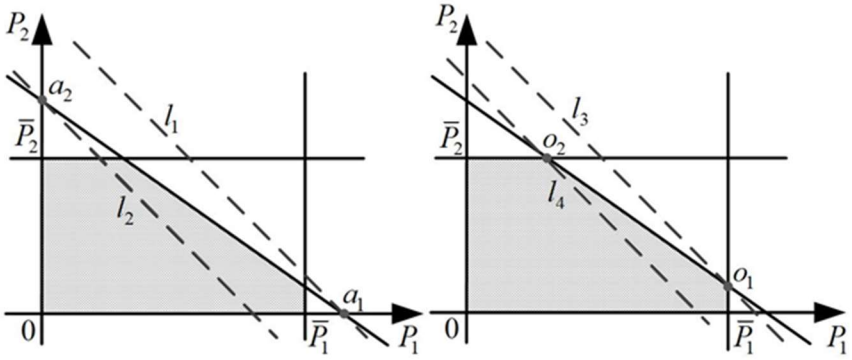

(a) Grouped constraints l_1 and l_2 (b) Grouped constraints l_3 and l_4

Figure 8: Illustration of the proposed variable grouping approach

2.3. Case Study

The analysis uses the grouping approach to obtain the quality of UC solutions and the accuracy of transmission flows.

2.3.1. UC Solution Analysis

Testing results of 10 cases are presented in Tables 5 and 6 against different similarity threshold ε_{SI}, which is used to cluster the master pnodes. A smaller similarity threshold means the SF vectors of master pnodes grouped in one cluster are more similar. The compression ratio (CR) is defined as the number of master pnodes over the number of similar pnodes, which reflects the degree of similarity and condensability of the original network security constraints. The speedup ratio (SR) is the solution time of SCUC with grouped network security constraints to the time of SCUC with the original network security constraints. Relative Gap (RGap) is calculated as the relative gap between the objective from Step 3 in Figure 7 and the best lower bound from SCUC with the original network security constraints (which is calculated by directly solving the full-SCUC with an optimization gap of 0.1%). To further perform sensitivity analysis of grouped SFs, two methods were developed to calculate the grouped SFs. In one method the grouped SFs could be viewed as the geometric average of the original coefficients of network security constraints, named as "Agg-SF-Geo," while in the other one the grouped SF's are calculated by the arithmetic average of the original coefficients, named as "Agg-SF-Ari."

Tables 5 and 6 show that with a larger similarity threshold ε_{SI}, both CR and SR are generally larger, while the solution quality becomes worse with higher RGap. In most cases, SR and RGap based on Agg-SF-Geo and Agg-SF-Ari are comparable. In addition, as the total grouping error increases with respect to a larger ε_{SI}, Agg-SF-Geo tends to perform better than Agg-SF-Ari in terms of both computational efficiency and solution quality. With large-scale and widespread DERs in cases 2.1 to 2.3, average values of CR, SR, and RGap are all larger than those from cases 1.1 to 1.7. It indicates that, when more nodes and resources with similar SFs are to be grouped, the proposed grouping method is more computationally efficient (i.e., with larger CR and SR) while the grouping error inevitably gets larger, resulting in relatively lower solution quality (i.e., larger RGap).

Case	ε_{SI}=0.01				
	Compression Ratio	Speedup Ratio		RGap (%)	
		Agg-SF-Geo	Agg-SF-Ari	Agg-SF-Geo	Agg-SF-Ari
1.1	1.39	1.94	2.08	0.097	0.109
1.2	1.37	1.67	1.88	0.072	0.075
1.3	1.38	1.8	1.81	0.09	0.097
1.4	1.38	5.49	1.91	0.115	0.101
1.5	1.37	5.86	6.95	0.089	0.095
1.6	1.37	11.1	14.3	0.112	0.126
1.7	1.37	1.98	1.71	0.114	0.108
Average	1.38	4.27	4.38	0.010	0.102
2.1	2.45	5.14	6.51	0.148	0.190
2.2	2.75	5.52	5.72	0.122	0.187
2.3	2.05	4.68	3.40	0.188	0.196
Average	2.42	5.11	5.21	0.153	0.191

Table 5: Testing results of the 10 cases with ε_{SI}=0.01

Case	ε_{SI}=0.03				
	Compression Ratio	Speedup Ratio		RGap (%)	
		Agg-SF-Geo	Agg-SF-Ari	Agg-SF-Geo	Agg-SF-Ari
1.1	1.87	5.22	3.65	0.280	0.138
1.2	1.85	1.76	1.94	0.119	0.099
1.3	1.88	2.12	2.67	0.343	0.226
1.4	1.87	7.06	6.05	0.356	0.689
1.5	1.85	8.95	7.13	0.239	0.203
1.6	1.92	15.5	16.6	0.248	0.112
1.7	1.91	2.27	2.06	0.125	0.115
Average	1.88	6.13	5.72	0.24	0.226
2.1	5.34	18.0	8.17	0.423	0.663
2.2	6.23	9.04	10.7	0.341	0.437
2.3	4.03	7.69	5.61	0.262	0.197
Average	5.20	11.6	8.16	0.342	0.432

Table 6: Testing results of the 10 cases with ε_{SI}=0.03

2.3.2. Accuracy of Transmission Flow Solution Analysis

In addition to the UC performance analysis, the study examines the quality of transmission flow from the solutions of Step 2 in Figure 7. The quality is estimated by two metrics: (i) flow MW deviation and (ii) flow deviation ratio. The flow MW deviation is calculated as:

$$(\text{Solved flow} - \text{Recalculated flow}), \text{ where}$$

$$\text{Solved flow} = \text{Aggregated SF} * \text{Solved MW}, \text{ and}$$

$$\text{Recalculated flow} = \text{Original SF} * \text{Solved MW}.$$

The flow deviation ratio is calculated as:

$$(\text{Solved flow} - \text{Recalculated flow})/\text{Original flow limit}.$$

These two metrics reflect the impact of grouping on the accuracy of transmission flow solutions. The average flow deviation with different similarity thresholds is presented in Table 7, and the detailed flow deviations for each line in whole periods are presented in Figure 9 and Figure 10. In Figure 9 and Figure 10, the two curves of the same color in the two subfigures (i.e., flow MW deviation and flow deviation ratio) correspond to the same transmission constraint. Large deviation ratios usually correspond to small flow limits. For example, the blue line in Figure 9(b) has a large deviation ratio in some intervals, which is caused by the flow limit changing from 475MW to 10MW. The lines with large deviation ratios in Figure 9 and Figure 10 suggest taking caution when processing the security constraints with relatively small limits, especially for the ones that could be easily binding. These constraints (though the number of these constraints cold be small) could be excluded from the grouping process, or grouped separately with a smaller similarity thresholds. From the graph, even with $\varepsilon_{SI} = 0.03$, the flow deviation can be over 100MW.

Similarity threshold ε_{SI}	Average flow deviation			
	Case A		Case B	
	MW deviation	Ratio	MW deviation	Ratio
$\boldsymbol{\varepsilon_{SI} = 0.01}$	1.54 (MW)	0.0098	3.03 (MW)	0.0123
$\boldsymbol{\varepsilon_{SI} = 0.02}$	8.82 (MW)	0.0478	6.29 (MW)	0.0427
$\boldsymbol{\varepsilon_{SI} = 0.03}$	12.39 (MW)	0.0828	12.02 (MW)	0.1080

Table 7: Average flow deviation with different similarity thresholds

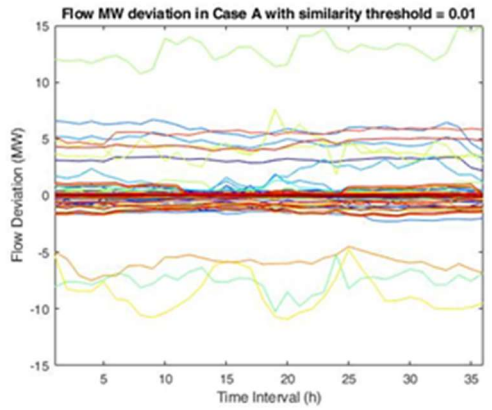

(a) Flow MW deviation with $\varepsilon_{SI} = 0.01$

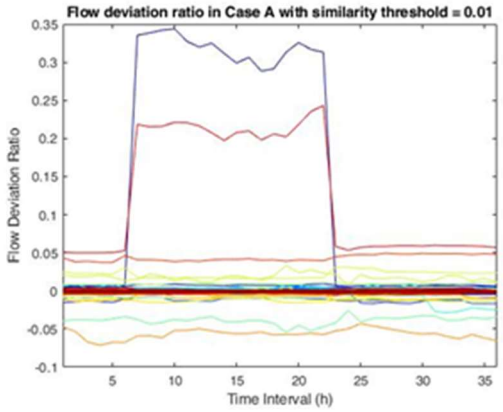

(b) Flow deviation ratio with $\varepsilon_{SI} = 0.01$

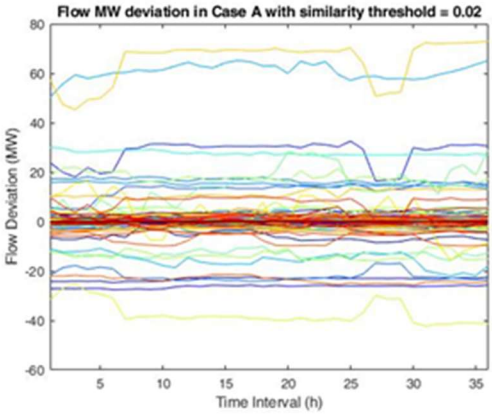

(c) Flow MW deviation with $\varepsilon_{SI} = 0.02$

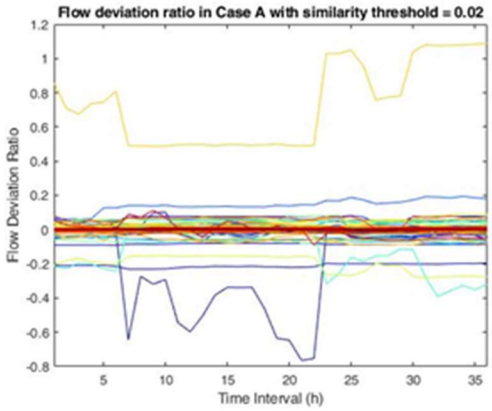

(d) Flow deviation ratio with $\varepsilon_{SI} = 0.02$

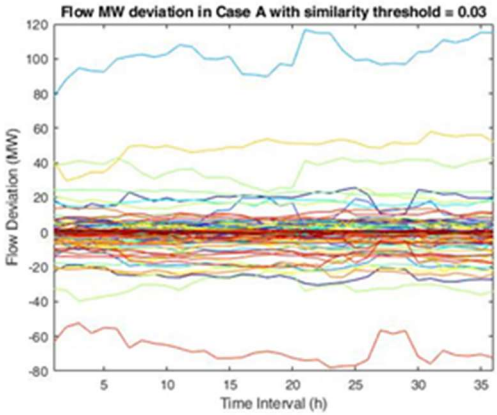

(e) Flow MW deviation with $\varepsilon_{SI} = 0.03$

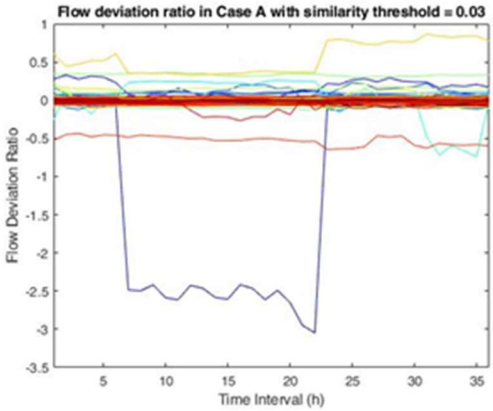

(f) Flow deviation ratio with $\varepsilon_{SI} = 0.03$

Figure 9: Flow deviation in Case A with different similarity thresholds

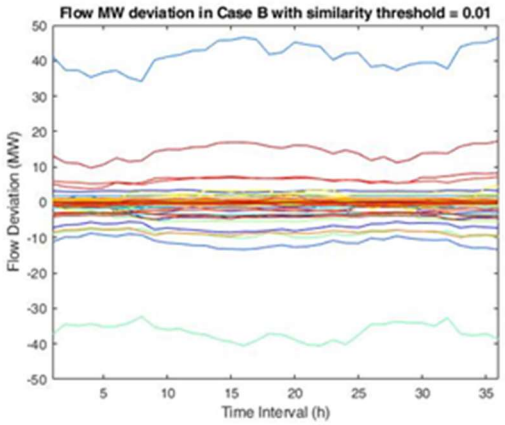

(a) Flow MW deviation with $\varepsilon_{SI} = 0.01$

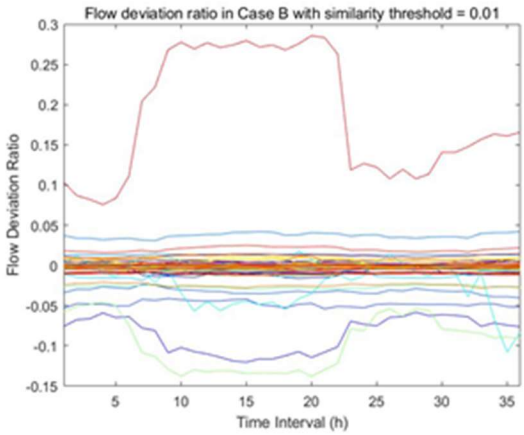

(b) Flow deviation ratio with $\varepsilon_{SI} = 0.01$

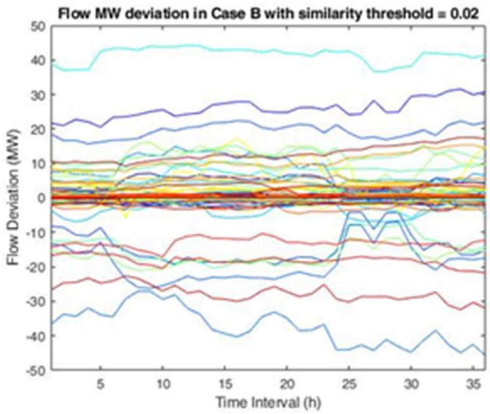

(c) Flow MW deviation with $\varepsilon_{SI} = 0.02$

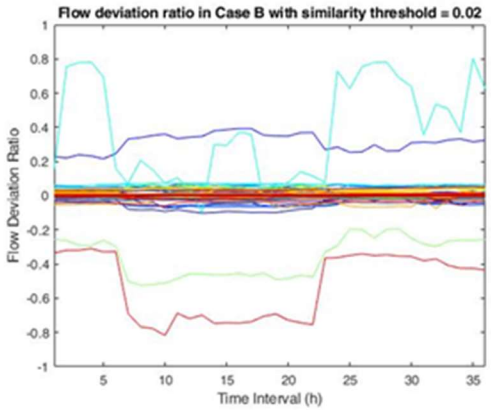

(d) Flow deviation ratio with $\varepsilon_{SI} = 0.02$

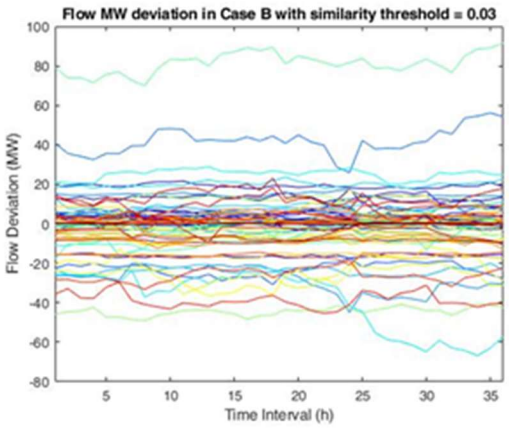

(e) Flow MW deviation with $\varepsilon_{SI} = 0.03$

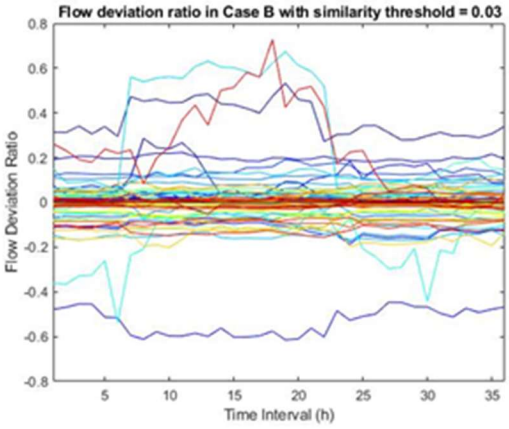

(f) Flow deviation ratio with $\varepsilon_{SI} = 0.03$

Figure 10: Flow deviation in Case B with different similarity thresholds

3. Projection-based Approaches for Transmission and Distribution Coordination

DERs are currently simplified as fixed or flexible loads in the wholesale energy market clearing, while the associated distribution networks are also neglected to achieve favorable computational features. However, in emerging distribution systems with an increasing penetration of DERs, this simplification would fail to precisely capture economic features of DERs and their impacts on distribution and transmission networks. To this end, two feasible region projection-based approaches are explored to optimally integrate high DER-penetrated distribution systems into the wholesale energy market clearing, while effectively capturing configuration details of distribution systems and fully respecting their internal physical limits (e.g., voltage and line flow constraints of distribution systems). The two approaches differ in terms of: (i) how the network constraints are simulated, and (ii) which variables are included in the wholesale energy market clearing model.

Specifically, Approach I[1] adopts the Θ-based method to formulate transmission and distribution network constraints. That is, the original transmission and distribution (T-D) system (as shown in Figure 11.a) can be decoupled by duplicating Θ and real power injections of the interconnection buses (as shown in Figure 11.b). With this, the feasible operation region of distribution systems can be projected as in Equation 2, where $\theta_{i,t}$ and $p_{i,t}$ are phase angles and real power injections at the T-D interconnection buses, and $p_{g,t}$ are dispatches of DERs. The major advantage of Approach I is that, because dispatches of individual DERs $p_{g,t}$ are kept in the projected distribution system constraints (Equation 2), their original bidding information can be directly used in the wholesale energy market model without approximation. The major disadvantage is that grid operators usually do not apply the Θ-based method to formulate network constraints, which induces significant variables and constraints for large-scale networks. Nevertheless, in the case of a single interconnection bus as shown in Figure 12, only one $p_{i,t}$ exists, which is solely determined by net load of the distribution side. Thus, $\hat{\theta}_{i',t} = \theta_{i,t}$ could be naturally managed, and $\theta_{i,t}$ is no longer needed to explicitly simulate the coupling between transmission and distribution systems. With this, the projected feasible region can be represented as in Equation 3, in which $\theta_{i,t}$ is no longer needed compared with Equation 2 and the transmission network can be switched to the shifting factor-based formulation.

$$\sum_{i\in\mathcal{I}_d^B} A_{h,i,t}^{\theta} \cdot \theta_{i,t} + \sum_{i\in\mathcal{I}_d^B} A_{h,i,t}^{P} \cdot p_{i,t} + \sum_{g\in\mathcal{G}_d^D} A_{h,g,t}^{G} \cdot p_{g,t} \le B_{h,t};$$

Equation 2

$$\sum_{i\in\mathcal{I}_d^B} A_{h,i,t}^{P} \cdot p_{i,t} + \sum_{g\in\mathcal{G}_d^D} A_{h,g,t}^{G} \cdot p_{g,t} \le B_{h,t};$$

Equation 3

[1] Y. Liu, L. Wu, Y. Chen, J. Li, Y. Yang, "On Accurate and Compact Model of High DER-Penetrated Distribution Systems in ISO Energy Market," IEEE Transactions on Sustainable Energy, vol. 12, no. 2, pp. 810-820, April 2021.

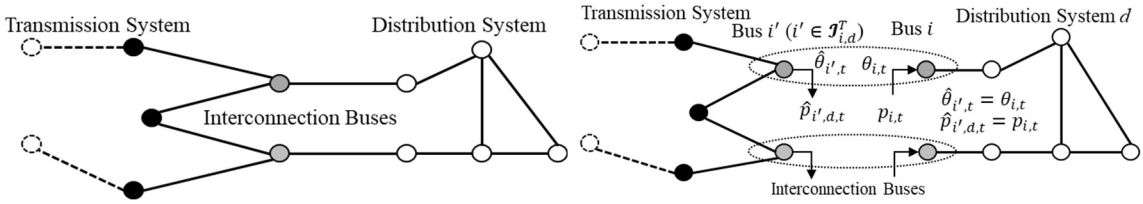

(a)Original T-D system (b) Variable duplication to represent T-D coupling

Figure 11: An illustrative example of variable duplication for a T-D system via Θ-based method

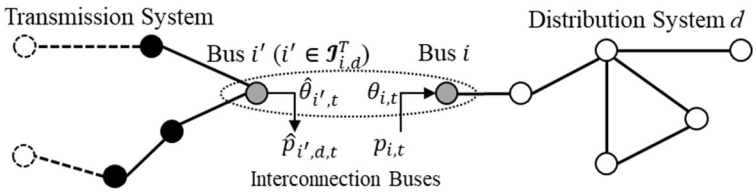

Figure 12: An illustrative example of a distribution system with a single interconnection bus

Approach II [2] adopts the shift factor (SF)-based method to formulate transmission and distribution network constraints. That is, the original T-D system (Figure 13.a) can be decoupled by duplicating real power injection variables at interconnection buses (Figure 13.b). With this, by building the SF matrix of the entire system (Figure 14), the feasible operation region of distribution systems can be projected as in Equation 4, where p_n are real power injections at the T-D interconnection buses. Using the SF matrix of the entire system as shown in Figure 14 could derive projected constraints more accurately. However, grid operators may not have the full network information. The proposed approach also works if the TT and DD submatrices are built independently. For example, TT may be built solely based on the transmission network while the distribution network information is not available to the transmission operator.DD for each distribution system may be built solely based on its network. However, missing TD and DT can potentially introduce higher power flows errors than the full SF. The major advantage of Approach II is that network constraints are formulated via the SF-based method, which is consistent with the current grid-operator practice. The major disadvantage is that as the projected distribution constraints (Equation 4) only include real power injections at the T-D interconnection buses, forcing reconstruction/approximation of bidding curves with respect to p_n based on the original bidding curves of DERs, which could introduce certain errors. A two-dimensional reconstructed bidding curve is shown in Figure 15, while the bidding curve with multiple interconnection buses would be more complicated.

$$\sum_{n \in \mathcal{N}} A_{h,n} \cdot p_n \leq B_h$$

Equation 4

[2] Y. Liu, L. Wu, Y. Chen, J. Li, "Integrating High DER-Penetrated Distribution Systems into ISO Energy Market Clearing: A Feasible Region Projection Approach," IEEE Transactions on Power Systems, DOI: 10.1109/TPWRS.2020.3028859, 2020.

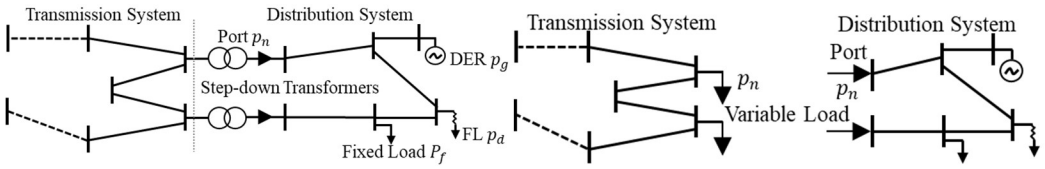

Original T-D system (b) Variable duplication to represent T-D coupling

Figure 13: An illustrative example of variable duplication for a T-D system via SF-based method

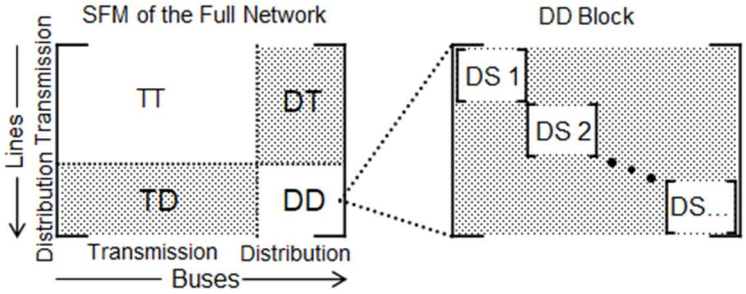

Figure 14: Structure of the SF matrix for the entire network

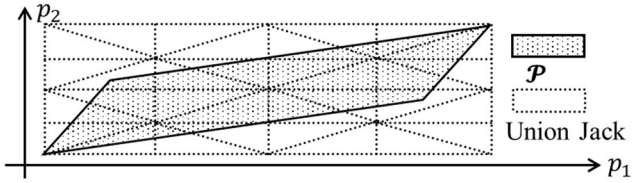

Figure 15: Reconstructing bidding curves with respect to $\mathbf{p_n}$.

The proposed algorithms were applied to an 1888-bus transmission system with multiple 33-bus distribution systems. Each distribution system includes eight DERs. Three test cases illustrate effectiveness of the proposed algorithms, which respectively include 5, 10, and 15 33-bus distribution systems. Three models are compared, including the full model that explicitly simulates all distribution system constraints in the UC model, the proposed projection-based approach, and the simplified model that mimics the grid operator's current practice that DERs in distribution systems directly bid at the interconnection buses (i.e., distribution network constraints are neglected, and power exchange between the transmission and distribution systems through multiple interconnection buses are not restricted by physical and operational limits of the distribution network). Results are compared in Table 8 where the proposed model derives more economic (i.e., the objective is closer to the full model) and secure (i.e., always feasible with respect to distribution system constraints) solutions than the simplified model, while is more computational effective than the full model.

Case	Full Model		Proposed Model		Simplified Model		
	Objective ($)	Time (s)	Objective ($)	Time (s)	Objective ($)	Time (s)	Distribution feasibility
Case 1	32,201,361	105.96	32,201,361	72.86	32,201,251	68.21	No
Case 2	32,204,066	145.35	32,204,066	77.31	32,203,842	69.28	No
Case 3	32,206,766	179.92	32,206,766	103.29	32,206,433	67.22	No

Table 8: Comparison of different cases

In addition, the projection-based approach can be considered as the nodal-based DER formulation (i.e., Epnode-based formulation), as compared to the aggregation-based formulation (i.e., Cpnode-based formulation) as discussed in Section 1. With this, as the physical interconnections of DERs to the transmission buses are exactly formulated and there is no need to approximate distribution factors of individual DERs, the LMP oscillation can be effectively avoided. Table 9 shows results of the same test case in Figure 5 of Section 1. The projection-based approach could introduce certain errors, as compared to the full model, while increasing the number of segments of the bidding curve may help reduce the errors (Table 10).

	Time	1	2	3	4	5	6	7	8
Real Time Economic Dispatch	Generator P_1 (MW)	100	100	100	100	100	100	100	100
	Generator P_2 (MW)	4.5	4.5	4.5	4.5	4.5	4.5	4.5	4.5
	DER_1 (MW)	0.7497	0.7497	0.7497	0.7497	0.7497	0.7497	0.7497	0.7497
	DER_2 (MW)	0.7502	0.7502	0.7502	0.7502	0.7502	0.7502	0.7502	0.7502
	Transmission flow (MW)	100.75	100.75	100.75	100.75	100.75	100.75	100.75	100.75
	LMP of bus 1 (MW)	8	8	8	8	8	8	8	8
	LMP of bus 2 (MW)	16	16	16	16	16	16	16	16

Table 9: Results of the test case in Figure 5 of Section 1

	Full Model	Proposed Model		
		3 segments	4 segments	5 segments
Generator P_1 (MW)	100	100	100	100
Generator P_2 (MW)	4.4792	4.5000	4.5000	4.5000
PD1 (MW)	0.7500	0.7497	0.7497	0.7496
PD2 (MW)	0.7708	0.7502	0.7503	0.7504
Obj ($)	685.92	686.50	686.25	686.12

Table 10: Dispatch results against different number of segments

4. Conclusions and Future Work

The following conclusions are derived based on this study:

(i) **Using the aggregation- (or approximation-) based model to aggregate small supply-side and demand-side resources at the Cpnode level may lead to unavoidable LMP oscillations.** This is large part due to DER responses deviating from the distribution factors used in the market clearing. This can cause efficiency and reliability concerns, with resources not being dispatched economically or transmission constraints being violated because of approximations.

(ii) **Use of a projection-based approach to model these resources at the Epnode level would avoid such LMP oscillation, guarantee feasibility of the distribution systems, and achieve sufficiently good dispatch solutions as compared to the ideal T-D co-optimization solution.** The projection-based approaches would need more information than the aggregation- (or approximation-) based model. Such information, including bidding price curves and physical constraints that describe economic and secure operations of the distribution systems with such resources, would need to be generated (via projection approaches) by the distribution system operators (DSO) and submitted to wholesale markets for market clearing.

(iii) **A grouping method could reduce the number of non-zero coefficients in network security constraints, and consequently mitigate computational burden of LP sub-problems in the MILP-based SCUC solution procedure.** In general, the grouping method could achieve fast calculation with sufficiently good SCUC solutions , even with a large number of DERs. When more nodes and resources with similar SFs are grouped, the grouping method is more computationally efficient. However, the solution quality could be compromised, resulting from the grouping error. Although the trade-off between computational efficiency and solution quality is unavoidable in the grouping method, testing results under high grouping accuracy is reasonable for getting sufficiently good unit commitment solution. However, even with 3% grouping error on shift factor, the flow deviation can be more than 100 MW and may result in real time dispatch issue and contribute to potential oscillation.

Because the proposed coordination approaches require more information and extra data exchange and model changes for grid operators, the team is further investigating whether alternate control strategies could avoid or mitigate oscillation while also deriving sufficiently good dispatch solutions. The team also continues to investigate alternative ways to improve computational performance through grouping and other techniques within the solution processes.

The team is contemplating the following aspects for future exploration:

(i) Although the preliminary tests illustrate that the projection-based Epnode-level model could potentially derive more economic and secure dispatch solutions than aggregating at the Cpnode-level, the EPnode-level model does require more information and extra efforts from both the grid operators to exchange data and modify models . As it is unclear which approach might be acceptable to handle the future scenario with a deeper penetration of DERs, the team plans to further investigate feedback control approaches (shown as the green box of Figure 16) on participation factors to avoid or mitigate LMP oscillation while also deriving sufficiently good dispatch solutions. Analysis indicates that the LMP oscillation would only be triggered under certain initial participation factor and system operation status. With this, the team plans to use fixed point method to explore sufficient conditions under which LMP oscillation could be avoided. Specifically, the Karush–Kuhn–Tucker (KKT) conditions of the RTED and the actual system operation model can derive two mappings: $DER\_RT = F(DF)$ and $DF = G(DER\_RT)$. These can then derive a mapping $DF_K + 1 = G\big(F(DF_k)\big) = M(DF_k)$, and use the contraction mapping theory to

analyze the convergence. As the mapping $F_K + 1 = M(DF_k)$ is mainly impacted by the incremental network constraints in the RTED as well as the distribution factor update equations, it is possible to explore other distribution factor update strategies, such as solving the least-squared problem to find a distribution factor value that leads to the best match between the RTED solution and the SE solution. The LMP oscillation work under Sections 1 and 3 is summarized in an IEEE conference paper.[3] Exploration of the fixed-point method-based theoretical studies could potentially resolve the LMP oscillation issues of the aggregation-based model.

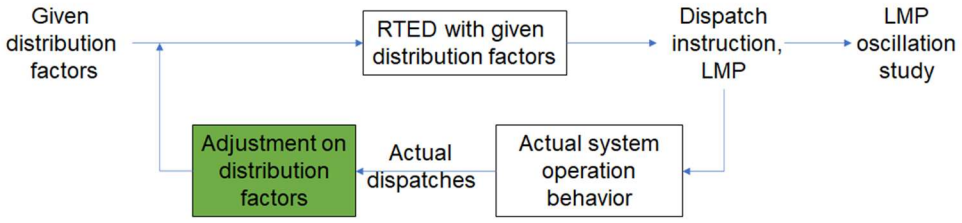

Figure 16: Feedback control-based scheme to explore sufficient conditions under which LMP oscillation could be avoided.

(i) The similarity between SFs of Epnodes in MISO system is not very high, which may limit effectiveness of the grouping method. To further address the performance issue of SCUC with significant DERs, there are plans to develop a variable reduction method by fixing part of resource variables, including DERs and generator units, based on the solution from relaxed mixed integer programming (RMIP). The preliminary testing results show this method could greatly reduce the solution time of SCUC by fixing partial resource variables. Besides, the RMIP solution may help construct better grouped network security constraints. With this, the numbers of resource variables and nonzero coefficients in network security constraints could be further reduced by the two approaches, and consequently the size of SCUC model to be solved by MILP solver will be smaller. To further improve computational performance, a series of reduced models will be generated and parallelly solved to obtain a good upper bound as fast as possible. The framework of the planned future work is shown in Figure 17. Complete related tests and technical details will appear in the journal paper[4] that is under preparation.

[3] K. Zuo, Y. Liu, J. Xia, Y. Yang, L. Wu, and Y. Chen, "Impact of Distributed Energy Resource Integration on Real-time Energy Market Oscillation", IEEE PES General Meeting, July 2021. Available online: https://drive.google.com/file/d/1e5q4A_pr5c-wtIlop139v4hmgHbDVty5/view.

[4] Y. Yang, L. Wu, Y. Chen, and Y. Liu, "Fast Day-Ahead SCUC for Integrating Large-Scale DERs into Wholesale Energy Market", under preparation.

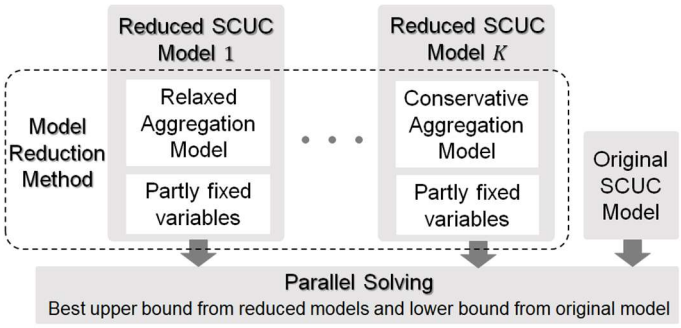

Figure 17: Framework of reduction methods for SCUC with DERs

5. References

Y. Liu, L. Wu, Y. Chen, J. Li, and Y. Yang, "On Accurate and Compact Model of High DER-Penetrated Distribution Systems in ISO Energy Market," IEEE Transactions on Sustainable Energy, vol. 12, no. 2, pp. 810-820, April 2021.

Y. Liu, L. Wu, Y. Chen, and J. Li, "Integrating High DER-Penetrated Distribution Systems into ISO Energy Market Clearing: A Feasible Region Projection Approach," IEEE Transactions on Power Systems, DOI: 10.1109/TPWRS.2020.3028859, 2020.

Y. Yang, X. Lu, and L. Wu, "Integrated Data-Driven Framework for Fast SCUC Calculation," IET Generation, Transmission & Distribution, vol. 14, no. 24, pp. 5728-5738, December 2020.

Y. Yang, L. Wu, Y. Chen, and Y. Liu, "Fast Day-Ahead SCUC for Integrating Large-Scale DERs into Wholesale Energy Market," under preparation.

K. Zuo, Y. Liu, J. Xia, Y. Yang, L. Wu, and Y. Chen, "Impact of Distributed Energy Resource Integration on Real-time Energy Market Oscillation," IEEE PES General Meeting, July 2021. Available online: https://drive.google.com/file/d/1e5q4A_pr5c-wtIlop139v4hmgHbDVty5/view.

L. Wu and Y. Chen, Day-Ahead SCUC for Integrating Large-Scale DERs into Wholesale Energy Market, FERC Technical Conference: Increasing Real-Time and Day-Ahead Market Efficiency and Enhancing Resilience through Improved Software, June 2020.